Theor Chim Acta (1986) 69: 281-307

Theoretica Chimica Acta

Bifurcations and transition states

Petros Valtazanos and Klaus Ruedenberg

Ames Laboratory, USDOE* and Department of Chemistry, Iowa State University, Ames, IA 50011, USA

(Received September 23, revised November 25/Accepted November 26, 1985)

Bifurcations of reaction channels are related to *valley-ridge inflection points* and it is examined what happens when these do not coincide with transition states. Under such conditions there result *bifurcating regions.* There exist a number of different prototypes for such regions which are discussed explicitly on the basis of the pertinent Taylor expansions. When bifurcations occur close enough to transition states then there result *bifurcating transition regions.* An example for a bifurcating transition region is exhibited which is obtained from a quantum mechanical *ab initio* calculation for the ring opening of cyclopropylidene to allene. In general there exist no orthogonal trajectory patterns which could serve as simplified models for channel bifurcations.

Key words: Chemical reactions — Potential energy surfaces — Reaction paths — Transition states — Bifurcations

1. The location of bifurcations

When C_s symmetry is lost during a reaction, then there must occur a bifurcation somewhere along the reaction path, because there exist *two products* which are transformed into each other by the C_s operation, whereas there is only *one reactant* which goes into itself under this operation [1]. Bifurcations also occur when C_2 or a higher symmetry is lost [2]. In many cases the reaction path starts out maintaining the C_s symmetry and one would then expect three possibilities as regards the bifurcation, namely that it could occur *before, at* or *after* the transition

* Operated for the U.S. Department of Energy by Iowa State University under Contract No. W-7405-ENG-82. This work was supported by the Office of Basic Energy Sciences

state. In the first case there exist of course two transition states which, too, are transformed into each other by the C_s operation. Indeed, it has been found that the transition state occurs before the bifurcation for the isomerizations $H_2CO \rightarrow HCOH$ and $H_3CO \rightarrow H_2COH$ [3, 4] and that the bifurcation occurs before the transition state for the isomerization $H_2CS \rightarrow HCSH$ [5], and for the exchange reaction $^{37}Cl + H^{35}Cl \rightarrow H^{37}Cl + {}^{35}Cl$ [6]. Miller [7] as well as Garrett, Truhlar, Wagner and Dunning [6] have discussed the simultaneous symmetric treatment of the dynamics along both reaction paths when the bifurcation occurs before the transition state. The ring opening of H_2CCCH_2 discussed in Sect. 6 is a case where the bifurcation occurs almost at the transition state.

The study of such energy surfaces leads to the question where on the reaction path a bifurcation should be perceived to take place. The dynamic trajectories cover a reaction channel and, in a certain region, this channel will divide into two branches. It would be convenient if one could locate such branching regions by examining the topography of energy surfaces without making dynamical calculations. One might think that information to this end could be obtained by looking for bifurcations or orthogonal trajectories on energy surfaces. It turns out, however, that *orthogonal trajectories are unsuited as reaction path models for the description of bifurcations.*

To be sure, bifurcations of orthogonal trajectories do exist, but their locations are severely restricted. To begin with, since such a bifurcation requires that several orthogonal trajectories emanate from one point in directions forming angles different from 180° with each other, it is apparent that *it can occur only when the gradient vanishes, i.e., at stationary points.* Indeed, all minima and maxima are "multifurcation" points, i.e. confluences of infinitely many orthogonal trajectories. For a *transition state* to be such a bifurcation point, it must have *downhill* trajectories forming angles other than 180° with each other. For an ordinary *second order* saddle point this would require the hessian to have at least two negative eigenvalues and, then, the saddle point would no longer be a transition state, because least energy paths circumvent second order saddle points with more than one negative eigenvalue of the hessian [8]. *For a transition state to be a bifurcation point of orthogonal trajectories, it is therefore necessary that the hessian has a zero eigenvalue at that point.* As a matter of fact, bifurcations of orthogonal trajectories are even more severely restricted. For in Sect. 3 it will be seen that they do *not* bifurcate at transition points where only *one* eigenvalue of the hessian vanishes. *The hessian must have at least two zero eigenvalues at a transition state for orthogonal trajectories to bifurcate at that point.* An example is the "monkey saddle"

$$E(x, y) = \tfrac{1}{3}ax^3 - xy^2, \qquad a > 0, \tag{1.1}$$

whose contours, together with some of the orthogonal trajectories given by

$$[(2+a)x^2 - y^2]y^a = \text{constant}, \tag{1.2}$$

are shown in Fig. 1. The orthogonal trajectories for constant = 0 consist of the three straight lines

$$y = 0, \qquad y = x\sqrt{2+a}, \qquad y = -x\sqrt{2+a}, \tag{1.3}$$

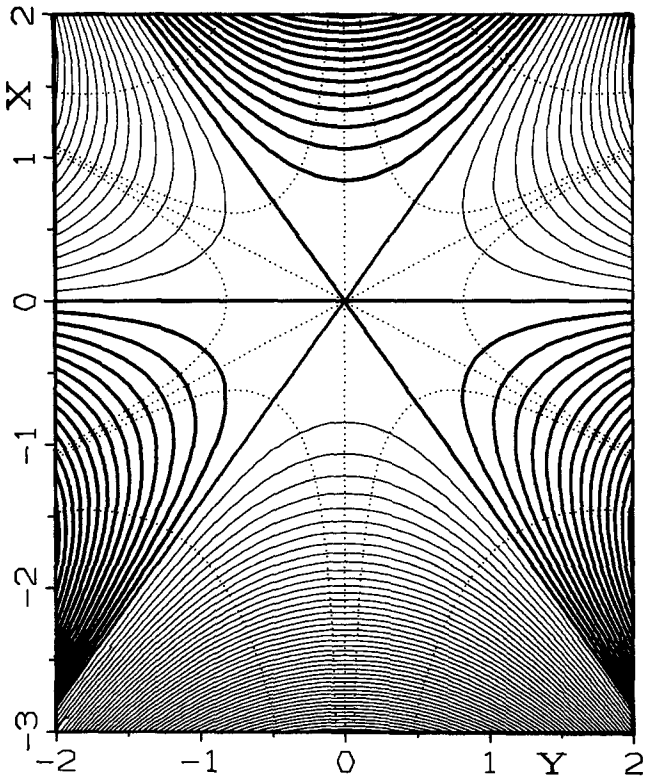

Fig. 1. The surface $E = 0.5x^3 - xy^2$. *Light solid lines*: contours for $E < 0$. *Heavy solid lines*: contours for $E \geq 0$. *Lowest heavy contour*: $E = 0$. Increment between *adjacent contours*: 0.3. *Dotted lines*: selected orthogonal trajectories

each of which changes from a valley floor to a ridge crest at the origin. Therefore the least energy orthogonal trajectory, coming up from one valley, splits up at the origin to descend into one or the other of the two valleys.

It will also become evident in Sect. 3 however that, in fact, transition states usually are points of bifurcation even if only *one* eigenvalue of the hessian vanishes there. And it will be seen in Sect. 4 that there exist surfaces which have bifurcating character in regions away from stationary points. *In none of these cases do there exist any least-energy orthogonal trajectories which bifurcate anywhere between reactants and products!*

For energy surfaces of actual physical systems it must be considered rather improbable, as several authors have pointed out [8], that an eigenvalue of the hessian vanishes exactly at a transition state because the latter is already completely determined by the vanishing of all first derivatives. The kind of bifurcation discussed in Sect. 3 is therefore expected to be a rare numerical accident. By the same token the monkey saddle, where *two* eigenvalues of the hessian vanish at the transition point, is *extremely* unlikely and one is thus led to the conclusion

that *least energy orthogonal trajectories split up "almost always" at minima, i.e., at those points on the energy surface which correspond to the reactants.*

On the other hand, there do exist reactions which start out along one channel and subsequently branch into two channels to reach two products. The energy surfaces discussed in Sects. 4 and 5 correspond to such cases. It is apparent from what has been said before that *there exist no orthogonal trajectory patterns onto which one can map such channel bifurcations.* The question arises therefore whether bifurcations can be located on energy surfaces without referring to orthogonal trajectories. This question is addressed in the present investigation.

We find an answer by focussing attention on the following fact: *If the path of a reaction at first follows a valley on the reaction surface and then comes to a point where the valley turns into a ridge, then the reaction path can be expected to bifurcate near that point* [9]. The reason is simple. Whereas the valley floor is a "stable path" in the sense that there exists a restoring force which tends to drive the trajectories of the system back to the floor, the crest of a ridge is an unstable path in as much as the slightest deviation of the system's trajectories will lead to their veering away further and further. Bifurcations are thus expected near *valley-ridge inflection points*, which we shall call VRI points.

We define VRI points as follows: *the hessian matrix has a zero eigenvalue and the corresponding eigenvector is perpendicular to the gradient at that point.* For the hessian to have a zero eigenvalue, its determinant must vanish, i.e.

$$E_{xx}E_{yy} - E_{xy}^2, \tag{1.4}$$

and this equation determines a curve in the (x, y) space. At any point on this curve the eigenvector with the zero eigenvalue is given by

$$N'\{E_{xy}, -E_{xx}\} = N''\{E_{yy}, -E_{xy}\}, \tag{1.5}$$

and for this eigenvector to be orthogonal to the gradient requires that

$$E_x E_{xy} - E_{xx}E_y = E_x E_{yy} - E_{xy}E_y = 0. \tag{1.6}$$

The intersections of the two curves defined by Eqs. (1.4) and (1.6) determine the VRI points. Since the gradient is parallel to the eigenvector with nonzero eigenvalue at such points, they lie on *gradient extremals* [10]. Indeed, for the surface discussed in Sect. 3.2 of the preceding paper [10], a VRI point was found at $(x = 0.685, y = 0.920)$ as shown by the vanishing of λ' on Fig. 4, by the contours on Fig. 2, and as commented upon at the end of Sect. 3.2 of that paper. On Fig. 2 of the preceding paper [10] the entrance channel separates in the two exit channels over a wide and flat region containing the VRI point which one can consider as the *bifurcation region.*

In the present investigation we are particularly interested in the case that the bifurcation region encompasses transition states so that one has a *bifurcating transition region.* Although, for the reasons given above, the exact coincidence of a transition state with a VRI point is expected to be a rare accident, near-coincidences seem to be less so. Indeed this investigation was prompted by the

discovery of such an approximate coincidence on the energy surface which will be discussed in Sect. 6. We shall examine the neighborhoods of valley-ridge inflection points on surfaces having C_s symmetry and we shall consider all possible cases under the condition that the hessian has only one vanishing eigenvalue at the VRI point.

The present analysis has also a practical application. It is apparent that the energy surface is very flat within a bifurcating transition region and that it is therefore difficult to determine the transition state and the VRI point accurately by standard second-order interpolation. The higher-order Taylor expansions discussed in the sequel furnish the appropriate interpolative tool under these circumstances, as will be illustrated in Sect. 6.

2. Energy surface in the neighborhood of a valley-ridge inflection point

Consider a reaction surface in terms of two internal coordinates, $E = E(x, y)$, which has C_s symmetry. When the system point lies on the line of symmetry, then the molecular system itself has C_s symmetry. If the system point does not lie on this line, then the molecule does not have C_s symmetry, but there then exists another system point, related to the first by the C_s reflection, which corresponds to the molecular geometry which is the mirror image of the previous one.

If the x-axis is chosen to be identical with the trace of the C_s symmetry plane in the $x-y$ plane, then one has $E(x,-y)=E(x,y)$ and the surface can be expressed in the form

$$E(x, y) = F(x, y^2). \tag{2.1}$$

On the C_s plane, i.e. for $y=0$, one has then

$$\partial E/\partial y = 0, \tag{2.2}$$

$$\partial^2 E/(\partial y)^2 = 2\,\partial F/\partial(y^2). \tag{2.3}$$

From Eq. (2.2) it is apparent that the surface is a valley or a ridge along the x-axis. Specifically,

$$\text{the } x\text{-axis is a valley (or a cirque), if } \partial F/\partial(y^2) > 0, \tag{2.4}$$

$$\text{the } x\text{-axis is a ridge (or a cliff), if } \partial F/\partial(y^2) < 0. \tag{2.5}$$

We are interested in the neighborhood of those points where *a valley* (*cirque*) *changes into a ridge* (*cliff*), i.e. where

$$\partial F/\partial(y)^2 = 0, \tag{2.6}$$

which we called *valley-ridge inflection* (VRI) *points.*

Without loss of generality, the origin, where $x=0$, may be placed at the VRI point whose neighborhood is of interest. Furthermore by adding an appropriate constant to E the zero of the energy surface can be shifted to the origin. Thus the conditions

$$F(x, y^2) = 0, \qquad \partial F/\partial(y)^2 = 0 \tag{2.7}$$

are valid at the origin $x=y=0$ and, hence, the expansion of F up to second order in x and y^2 around the origin has the form

$$E(x, y) = F(x, y^2) = A_1 x + A_2 x^2 + 2A_3 x y^2 + A_4 y^4. \tag{2.8}$$

The first and second derivatives of this function are

$$E_x = A_1 + 2A_2 x + 2A_3 y^2, \tag{2.9a}$$

$$E_y = 4y(A_3 x + A_4 y^2), \tag{2.9b}$$

$$E_{xx} = 2A_2, \tag{2.9c}$$

$$E_{yy} = 4A_3 x + 12A_4 y^2, \tag{2.9d}$$

$$E_{xy} = 4A_3 y. \tag{2.9e}$$

The eigenvalues of the hessian at the VRI point are 0 and $2A_2$. Since we assume one eigenvalue to be non-zero we must have $A_2 \neq 0$ and this justifies the neglect of terms in x^3 and x^4 in Eq. (2.8).

In the present context we are interested in *transition states* and this corresponds to the case that *on the x-axis*, where $E = A_1 x + A_2 x^2$, the surface has a *maximum*, implying that *the value of A_2 is negative*. We further assume that for large negative x-values we start in a *valley* on the x-axis. In view of the choice of the origin this implies that the x-axis is a valley for $x<0$ and a ridge for $x>0$. Since, according to Eq. (2.9d) one has $E_{yy} = 2A_3 x$ on the x-axis, it follows furthermore that *the value of A_3 is also negative*. Thus we consider only the case

$$A_2 < 0, \qquad A_3 < 0. \tag{2.10}$$

The value of A_1 determines the position of the maximum on the x-axis. This maximum occurs for

$$x_m = -A_1/2A_2, \tag{2.11}$$

at which point the energy surface assumes the value

$$E_m = -A_1^2/4A_2. \tag{2.12}$$

If A_1 is positive (case 3 below), then the point $(x_m, 0)$ lies on the ridge part of the x-axis and is a true (relative) maximum of the surface since, according to Eqs. (2.9c, d, e) one has $E_{xx}<0$, $E_{yy}<0$, $E_{xy}=0$ at this point. On the other hand, if A_1 is negative (case 2 below), then this point lies in the valley part of the x-axis and it is a saddlepoint, since Eqs. (2.9c, d, e) now yield $E_{xx}<0$, $E_{yy}>0$, $E_{xy}=0$. If the value of A_1 vanishes (case 1), then the point $(x_m, 0)$ lies at the origin and is a higher order point, a kind of saddle where, however, the valley changes into a ridge.

The value of A_4 determines the shape of the function contours in a more complicated manner which will be the object of the subsequent sections. The domain of A_4 is conveniently divided into five regions. These five cases are characterized in Table 1. In the cases (a), (b), (c), (d), i.e. for $A_4 \geq A_3^2/A_2$, it is also useful to express the function $E(x, y)$ in the form

$$E(x, y) = ax - b(x + c_1 y^2)(x + c_2 y^2), \tag{2.13}$$

Table 1. Five cases for the surface defined by Eqs. (2.8) and (2.13)

Case	Regions of A_4	Regions of c_1 and c_2
(a)	$A_4>0$	$c_1>0,\ c_2<0;\ c_1+c_2=2A_3/A_2>0$
(b)	$A_4=0$	$c_1=2A_3/A_2>0,\ c_2=0$
(c)	$0>A_4>A_3^2/A_2$	$c_1>0,\ c_2>0;\ c_1+c_2=2A_3/A_2$
(d)	$A_4=A_3^2/A_2$	$c_1=c_2=A_3/A_2$
(e)	$A_4<A_3^2/A_2$	complex

Note that A_3 and A_2 are both negative (see Eq. 2.10)

where the coefficients are related to those of Eq. (2.8) by the relations

$$A_1=a, \qquad A_2=-b, \qquad 2A_3=-b(c_1+c_2), \qquad A_4=-bc_1c_2, \tag{2.14}$$

$$c_1=(A_3-\sqrt{A_3^2-A_2A_4})/A_2, \qquad c_2=(A_3^2+\sqrt{A_3^2-A_2A_4})/A_2. \tag{2.15}$$

It is apparent that Eq. (2.10) implies

$$b>0, \qquad c_1+c_2>0. \tag{2.16), (2.17}$$

The behavior of c_1 and c_2 for the five cases (a) to (d) is shown in the last column of Table 1. Each of these five possible cases for A_4 has to be combined, of course, with the aforementioned three possible cases for A_1.

Equation (2.13) can also be written in the factored form

$$E=E_0-B(x+c_1y^2-x_1)(x+c_2y^2-x_2), \tag{2.18}$$

where the constants E_0, x_1, x_2 are defined by

$$E_0=(1-\gamma^2)E_m, \qquad x_1=(1+\gamma)x_m, \qquad x_2=(1-\gamma)x_m, \tag{2.19}$$

with E_m and x_m being the quantities given by Eqs. (2.11), (2.12) and γ being defined by

$$\gamma=(c_1+c_2)/(c_1-c_2). \tag{2.20}$$

It is apparent that the contour corresponding to the energy value $E=E_0$ consists of the union of the two parabolas

$$x=x_1-c_1y^2 \quad \text{and} \quad x=x_2-c_2y^2. \tag{2.21}$$

Finally we comment briefly on a subtlety. For the surface of Eq. (2.8) the x-axis is also a gradient extremal [10] as can be readily verified from Eq. (3.3) of [10]. One can therefore make the distinction between a valley and a cirque, and that between a ridge and a cliff (Sect. 2.2 of [10]). By virtue of the discussion in Sect. 3.1 of [10] the following is readily verified. At the VRI point a valley turns into a ridge when $A_1<0$ (bifurcation after transition state) and this is confirmed by the contour diagrams shown in Sect. 4. On the other hand, a cirque turns into a cliff at the VRI point when $A_1>0$ (bifurcation before transition state) and this is confirmed by the figures in Sect. 5. For simplicity we shall nonetheless continue to use the word "valley" to imply a valley or a cirque, and the word "ridge" to imply a ridge or a cliff.

3. First case: bifurcation at transition state

Whereas it was no loss of generality to place the origin at the VRI point, it cannot be expected in general that one has also E_x $(x=0, y=0) = A_1 = 0$ at this same point, i.e. that the origin is a stationary point as well as a VRI point. In the spirit of the arguments quoted in Sect. 1 such a coincidence would be considered as "unlikely". Nonetheless it is of interest to discuss this case first, before considering the general case of nonvanishing A_1. If $A_1 = a$ vanishes in Eq. (2.13) then we can, with no loss of generality, consider the prototype function

$$E(x, y) = -(x + c_1 y^2)(x + c_2 y^2). \tag{3.1}$$

On the x-axis, the maximum occurs at the origin, where $E = 0$. It is apparent that the contours going through the origin are given by the two parabolas

$$x + c_1 y^2 = 0 \quad \text{and} \quad x + c_2 y^2 = 0. \tag{3.2}$$

Figure 2 displays the contours for case $(1a)$, i.e. when c_1 and c_2 have opposite signs $(A_4 > 0)$, together with some typical orthogonal trajectories. The $-x$ axis is seen to be the bottom of a valley which ascends to the origin. The descent into the $+x$ direction is along a ridge. The contours that go through the origin, i.e. $E(x, y) = 0$, are the two parabolas of Eq. (3.2) that touch at the origin. The surface ascends in all directions that lie *between* these two parabolas. The origin has thus the character of a transition state. Since the descent into the $+x$ direction is along a ridge, a reacting system that has come up the valley from the $-x$ direction, will fall off this ridge soon after passing through the transition state.

For the special case where $c_1 = -c_2$ the contours and orthogonal trajectories are those shown in Fig. 3. The ridge on the $+x$ axis has disappeared in agreement with the fact that now $E_{yy} = 0$ everywhere on the x-axis (see Eq. 2.9d). The surface has now the simple form

$$E(x, y) = -x^2 + c_1^2 y^4, \tag{3.3}$$

and the origin is similar to an ordinary saddlepoint that lies at the intersection of two orthogonal trajectories, one connecting two valleys, the other connecting two ridges. But in contrast to a second order saddlepoint, the contours passing through the saddle are tangent to each other rather than intersecting with a finite angle. This case corresponds to $A_3 = 0$ which we had actually excluded in Sect. 2.

Figure 4 displays the contours and some orthogonal trajectories for case $(1c)$ i.e. when c_1 and c_2 are both positive $(A_3^2/A_2 < A_4 < 0)$. The main difference to Fig. 2 is that one of the parabolic contours going through the transition state has reversed its curvature. It is the one corresponding to c_2. As before the surface ascends uphill from the transition state in all directions *between* the two parabolic contours passing through the transition state. As before the $-x$ direction is an ascending valley. As before the $+x$ axis is a descending ridge, so that the origin is again a bifurcation point.

Intermediate between the cases $(1a)$ and $(1c)$ is case $(1b)$ corresponding to $A_4 = 0$ and $c_2 = 0$, so that

$$E(x, y) = -(x + c_1 y^2)x. \tag{3.4}$$

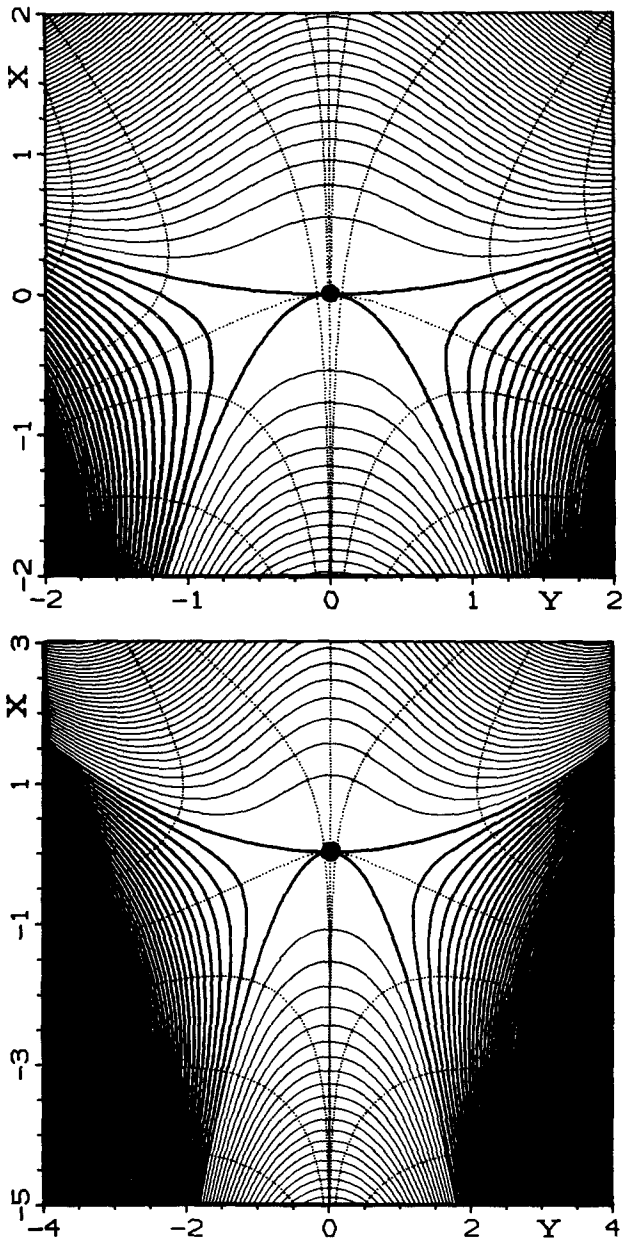

Fig. 2. The surface $E = -(x+1.5y^2)(x-0.1y^2)$. The top panel is an enlargement of the region near the VRI point which is identified by a *heavy dot. Light solid lines*: contours for $E < 0$. *Heavy solid lines*: contours for $E \geq 0$. *Lowest heavy contour*: $E = 0$. Increment between *adjacent contours*: 1.2 on lower panel, 0.3 on upper panel. *Dotted lines*: selected orthogonal trajectories

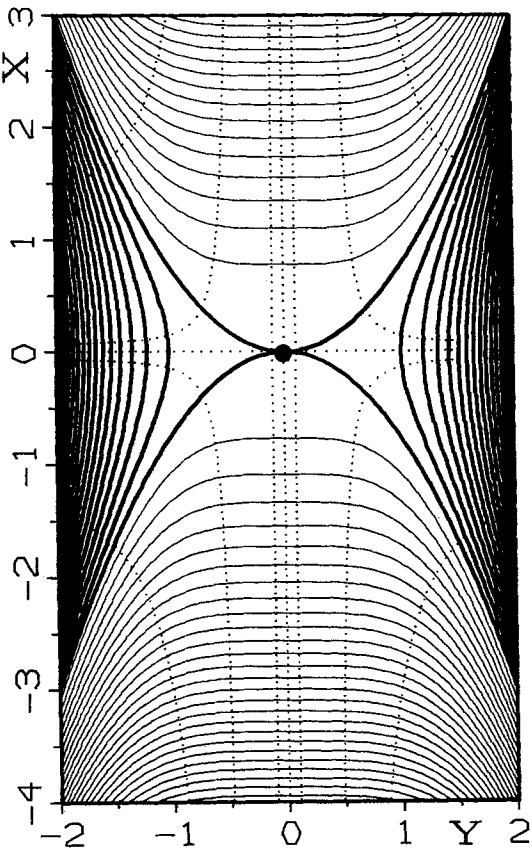

Fig. 3. The surface $E = -(x+0.75y^2) \times (x-0.75y^2)$. *Light solid lines*: contours for $E < 0$. *Heavy solid lines*: contours for $E \geq 0$. *Lowest heavy contour*: $E = 0$. Increment between *adjacent contours*: 0.6. *Dotted lines*: selected orthogonal trajectories

It is apparent that, now, one of the contours passing through the transition state is the y-axis, indeed intermediate between Figs. 2 and 4.

In all these cases there clearly are two exit channels, one on each side of the positive x-axis, even though they look more like watersheds than like valleys. It should be noted that *neither one of these exit channels contains any orthogonal trajectory that connects with the transition state or the entrance channel.* The only orthogonal trajectory that passes from the entrance channel into the half-plane $x > 0$ is the x-axis and it separates the two exit channels. All other orthogonal trajectories, even those very close to the x-axis, make a sharp left or right turn after passing the contour $E = 0$ and keep going uphill. It is thus apparent that *there exist no orthogonal trajectories which could serve as a simplified skeleton pattern for the bifurcation.* It is to this fact that we referred in the introduction.

Figure 5a exhibits the contours and some orthogonal trajectories for case (1*d*) corresponding to $A_3^2 = A_2 A_4$ or, alternatively, $c_1 = c_2 > 0$. The two parabolic contours passing through the origin coincide and the ridges going uphill from the transition state disappear. It is apparent from Eq. (3.1) that all contours are parabolas $(x + c_1 y^2) = \text{const}$. However, all contours have $E \leq 0$ so that the value of E *decreases* in *both* the $+x$ and $-x$ direction. One still has a valley on the $-x$

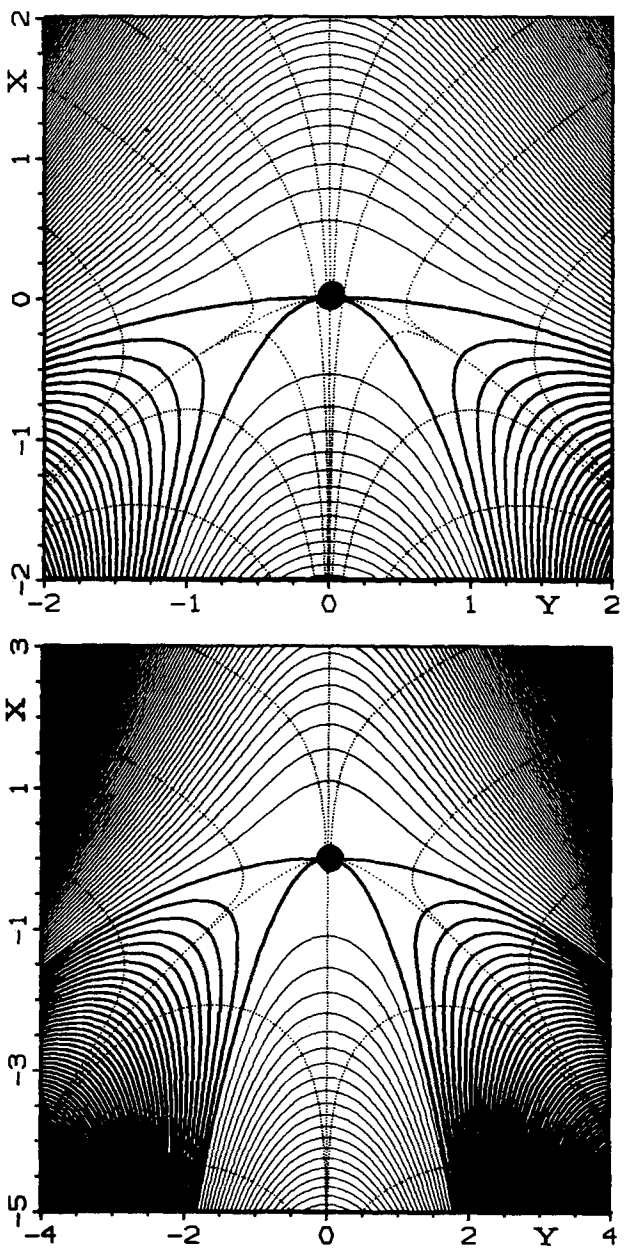

Fig. 4. The surface $E = -(x+1.5y^2)(x+0.1y^2)$. The *top panel* is an enlargement of the area near the VRI point which is identified by a *heavy dot. Light solid lines*: contours for $E < 0$. *Heavy solid lines*: contours for $E \geq 0$. *Lowest heavy contour*: $E = 0$. Increment between *adjacent contours*: 1.2 on lower panel, 0.3 on upper panel. *Dotted lines*: selected orthogonal trajectories

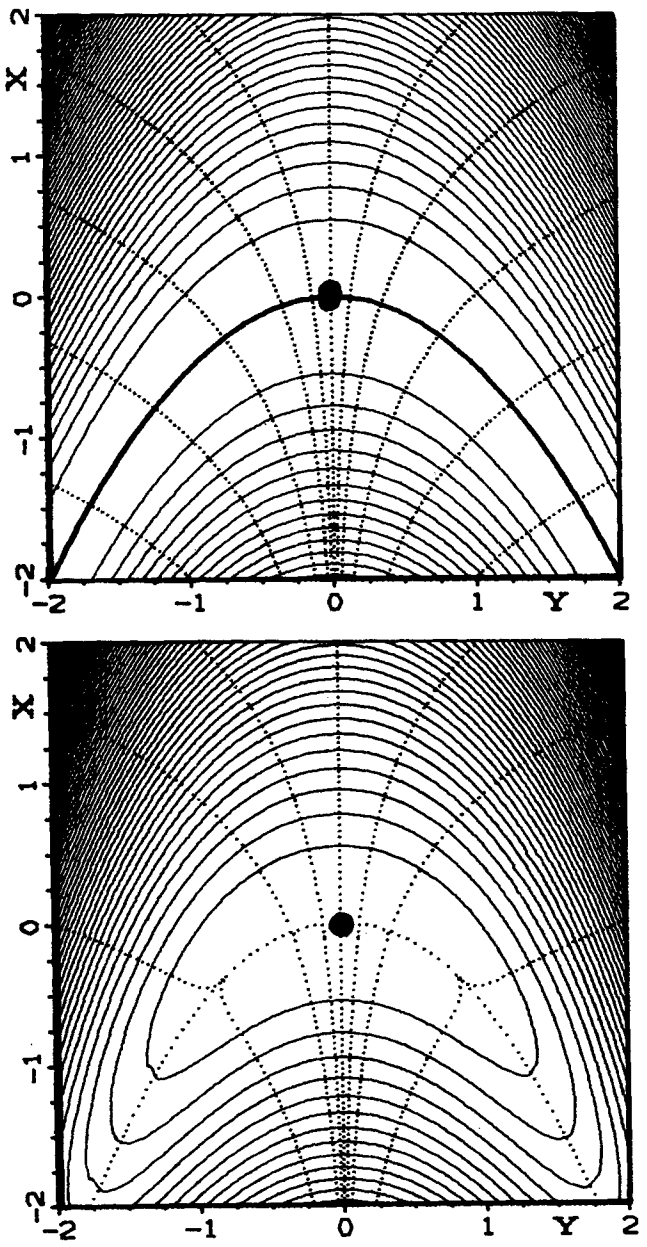

Fig. 5. *Upper panel*: the surface $E=-(x+0.5y^2)^2=-(x^2+xy^2+0.25y^4)$. *Lower panel*: the surface $E=-(x^2+xy^2+0.333y^4)$. *Light solid lines*: contours for $E<0$. *Heavy solid line*: contour for $E=0$. Increment between adjacent contours: 0.3. *Dotted lines*: selected orthogonal trajectories

axis and a ridge on the $+x$ axis. The origin is still a VRI point. But the *entire* contour $x + c_1 y^2 = 0$ represents the transition state.

Figure 5b exhibits the contours and some orthogonal trajectories for case (1*e*) where $A_4 < A_3^2/A_2$. It is still true that we have a valley on the $-x$ axis and a ridge on the $+x$ axis. The origin is still a VRI point, but the origin is a maximum not a transition state.

4. Second case: transition state before bifurcation

As discussed in the text after Eq. (2.12), there exists a saddlepoint on the negative x-axis when A_1 is negative. It is now expedient to choose the distance of this saddlepoint from the origin ($|x_m| = A_1/2A_2$, Eq. 2.11) as unit of length and the value of E at the saddlepoint ($-A_1^2/4A_2$, Eq. 2.12) as unit of energy. Through this choice of units the general expression (2.13) assumes the form

$$E(x, y) = -2x - (x + c_1 y^2)(x + c_2 y^2), \tag{4.1}$$

where $c_k(\text{new}) = |2A_2/A_1| c_k(\text{old})$.

Figure 6 exhibits the contours and orthogonal trajectories for case (2*a*) where c_1 and c_2 have opposite signs ($A_4 > 0$). The difference to case (1*a*), where $A_1 = 0$ is that the transition state has separated from the VRI point at the origin. The transition state is the saddlepoint at $x = -1$. Coming up the valley from $-x$, the reaction path reaches this saddlepoint and then descends in a short valley towards the origin, where the valley turns into a ridge.

In the special case where $c_1 = -c_2$, one has again $E_{yy} = 0$ on the entire x axis (see Eq. 2.9d). The resulting surface

$$E = -2x - x^2 + c_1^2 y^4 \tag{4.2}$$

differs from that of Eq. (3.3) only by the shift of the maximum to $x = -1$. The contours can therefore be obtained from those of Fig. 3 by a corresponding shift along the x-axis and increasing all contour values by adding 1.0.

Figure 7 shows the contours and orthogonal trajectories for case (2*c*) where c_1 and c_2 are both positive ($A_3^2/A_2 < A_4 < 0$). The differences in the contours between Figs. 6 and 7 are similar to those between Figs. 2 and 4. Everything that has been said for Fig. 6 also applies to Fig. 7.

If the distance between the saddlepoint and the valley ridge inflection point, on either of these surfaces, is short compared to the overall length of the reaction path and if, in addition, the energy difference between these two places on the surface is small compared to their elevation over the reactant and product energies, then it is justified to consider the region encompassing both, the saddlepoint and the valley ridge inflection point, as a *bifurcating transition region*. For all intents and purposes, the bifurcation of the reaction path occurs immediately after passing through the saddle.

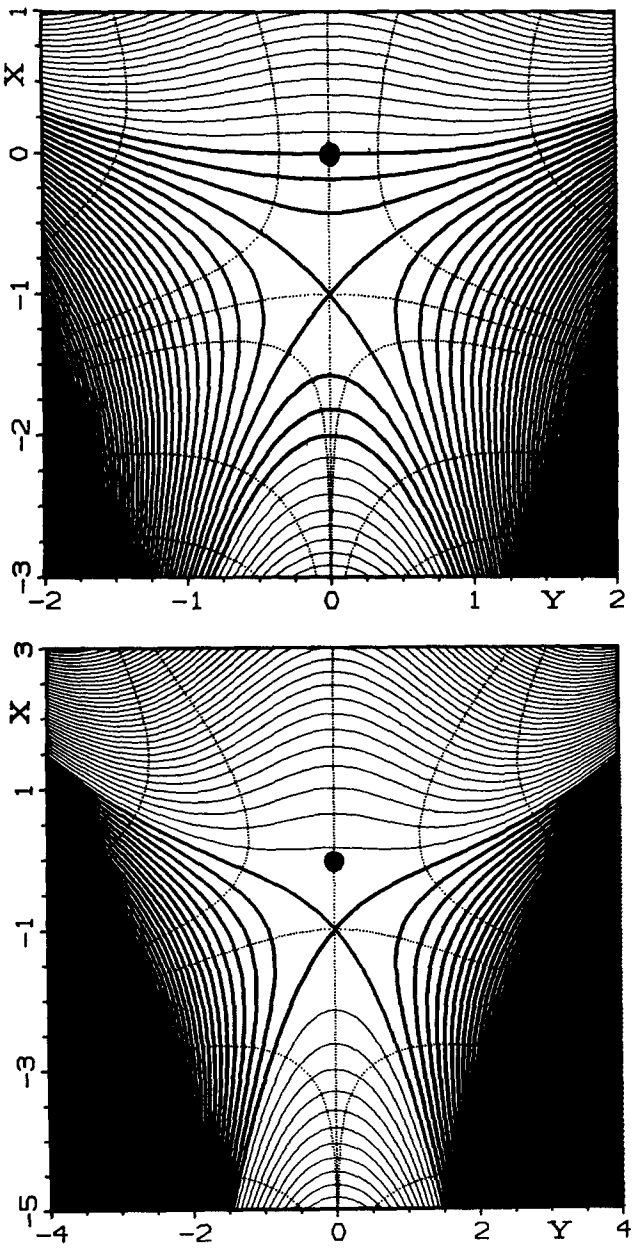

Fig. 6. The surface $E = -2x - (x + 1.5y^2)(x - 0.1y^2)$. The *top panel* is an enlargement of the region near the VRI point which is identified by a *heavy dot*. *Light solid lines*: contours for $E < 0$. *Heavy solid lines*: contours for $E \geq 0$. *Lowest heavy contour*: $E = 0$. Increment between *adjacent contours*: 1.333 ... on lower panel, 0.333 ... on upper panel. *Dotted lines*: selected orthogonal trajectories

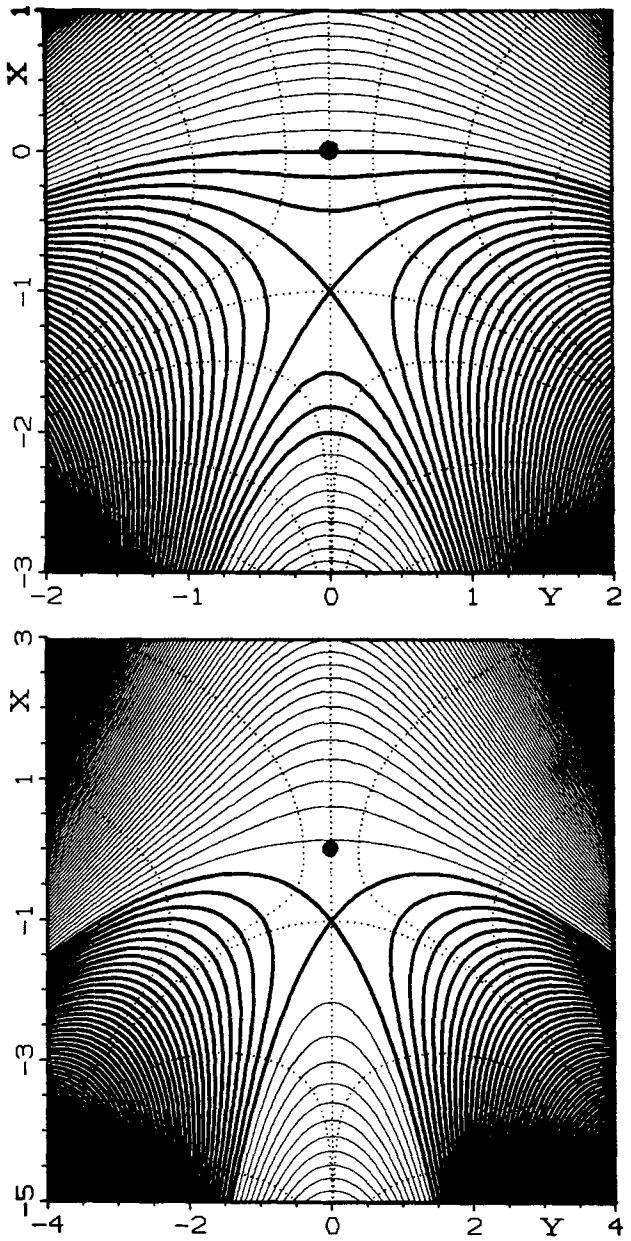

Fig. 7. The surface $E = -2x - (x + 1.5y^2)(x + 0.1y^2)$. The *top panel* is an enlargement of the region near the VRI point which is identified by a *heavy dot*. *Light solid lines*: contours for $E < 0$. *Heavy solid lines*: contours for $E \geq 0$. *Lowest heavy contour*: $E = 0$. Increment between *adjacent contours*: 1.333 ... on lower panel, 0.333 ... on upper panel. *Dotted lines*: selected orthogonal trajectories

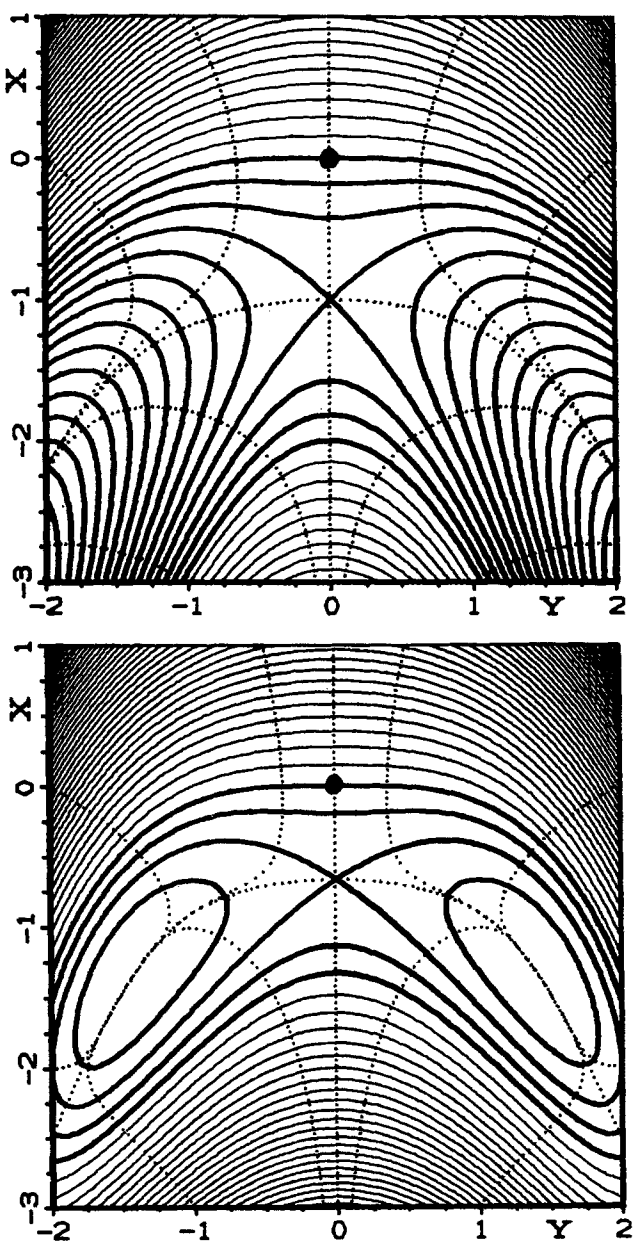

Fig. 8. *Upper panel*: the surface $E = -2x - (x + 0.5y^2)^2 = -(2x + x^2 + xy^2 + 0.25y^4)$. *Lower panel*: the surface $E = -(2x + x^2 + xy^2 + 0.333\ldots y^4)$. *Light solid lines*: contours for $E < 0$. *Heavy solid lines*: contours for $E \geq 0$. *Lowest heavy contour*: $E = 0$. Increment between *adjacent contours*: 0.333.... *Dotted lines*: selected orthogonal trajectories

Intermediate between the cases $(2a)$ and $(2c)$ is case $(2b)$ where $A_4=0$ and $c_2=0$, so that

$$E(x, y)=-x(2+x+c_1y^2). \tag{4.3}$$

It is apparent that, now, the contour passing through the VRI point is the y-axis, indeed intermediate between Figs. 6 and 7.

As was the case in the preceding section, neither one of the two exit channels contains any orthogonal trajectory that connects with the VRI point or the transition state or the entrance channel. The only orthogonal trajectory that passes from the entrance channel into the half-plane $x>0$ is the x-axis. It is a valley in the entrance channel and from the transition state to the VRI point. From there on out, it is a ridge that separates the exit channels. As before, there exist no orthogonal trajectories which could serve as a simplified pattern for modelling the bifurcation.

Figure 8a exhibits the contours for the case $(2d)$, corresponding to $A_3^2=A_2A_4$ and $c_1=c_2>0$. Figure 8b exhibits the contours for the case $(2e)$, corresponding to $A_4<A_3^2/A_2$. In both cases there still exists a saddlepoint. In case $(2e)$ the whole saddlepoint region can however be circumvented.

5. Third case: transition state after bifurcation

As discussed in the text after Eq. (2.12), the maximum on the x-axis occurs for a positive x value when A_1 is positive. It is furthermore a relative maximum in every direction. As in the preceding section, it is expedient to use its distance from the origin ($x_m=-A_1/2A_2$, Eq. 2.11) as unit of length and to choose the energy difference between the maximum and the origin ($-A_1^2/4A_2$, Eq. 2.11) as unit of energy. Thereby the energy surface assumes the form

$$E(x, y)=2x-(x+c_1y^2)(x+c_2y^2). \tag{5.1}$$

Figure 9 displays the contours and orthogonal trajectories of a surface of case $(3a)$ where c_1 and c_2 have opposite signs ($A_4>0$). Figure 10 displays the contours and orthogonal trajectories for case $(3c)$ where c_1 and c_2 are both positive ($A_3^2/A_2<A_4<0$). It is seen that, in both cases, the surface has two saddlepoints *off* the x-axis. The positions of these saddlepoints are obtained by using, in the stationary condition $E_x=E_y=0$, the derivative expressions (2.9a), (2.9b) in conjunction with the surface of Eq. (5.1). Assuming that y does not vanish, one thereby obtains the equation set

$$2x+(c_1+c_2)y^2=1, \tag{5.2a}$$

$$(c_1+c_2)x+2c_1c_2y^2=0, \tag{5.2b}$$

which has the solution

$$x_s=1-\gamma^2, \qquad y_s^2=\gamma^2/c, \tag{5.3}$$

where

$$\gamma=(c_1+c_2)/(c_1-c_2), \qquad c=(c_1+c_2)/2. \tag{5.4}$$

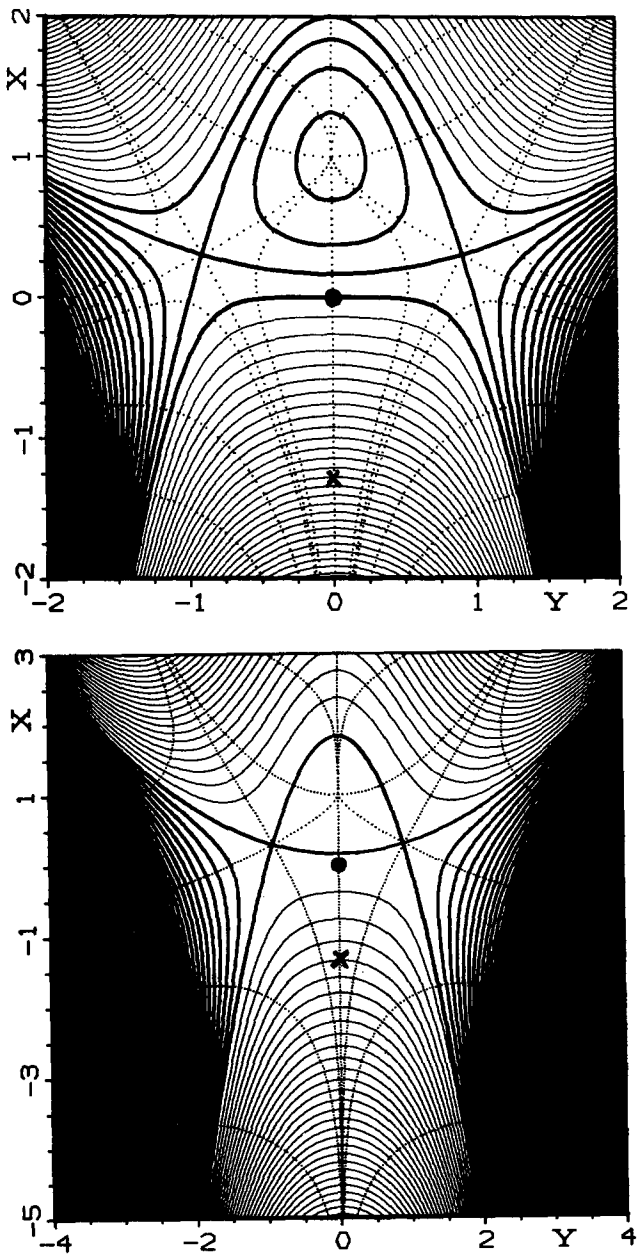

Fig. 9. The surface $E = 2x - (x + 1.83666y^2)(x - 0.16334y^2)$. The *top panel* is an enlargement of the region near the VRI point which is identified by a *heavy dot. Light solid lines*: contours for $E < 0$. *Heavy solid lines*: contours for $E \geq 0$. *Lowest heavy contour*: $E = 0$. Increment between adjacent contours: 1.2 on lower panel, 0.3 on upper panel. *Dotted lines*: selected orthogonal trajectories

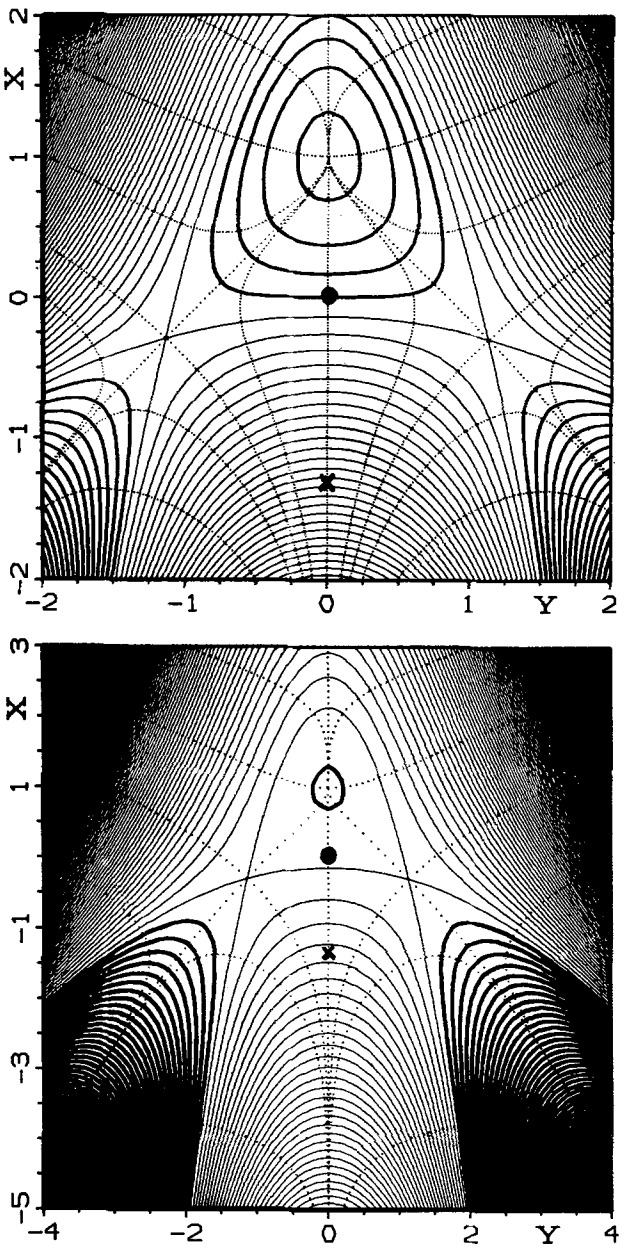

Fig. 10. The surface $E = 2x - (x + 1.87706y^2)(x + 0.12294y^2)$. The *top panel* is an enlargement of the region near the VRI point which is identified by a *heavy dot*. *Light solid lines*: contours for $E < 0$. *Heavy solid lines*: contours for $E \geq 0$. *Lowest heavy contour*: $E = 0$. Increment between *adjacent contours*: 1.2 on lower panel, 0.3 on upper panel. *Dotted lines*: selected orthogonal trajectories

It should be noted that both, γ and c, are positive in all cases. Hence, one has indeed two real stationary points, corresponding to $y_s = \pm\gamma/\sqrt{c}$. For c_1 and c_2 both positive, one has $\gamma > 1$ and hence $x_s < 0$; for $c_1 > 0$, $c_2 < 0$ (but $c_1 > |c_2|$), one has $\gamma < 1$ and hence $x_s > 0$, in agreement with Figs. 9 and 10. The value of the surface at the saddlepoints is found to be

$$E_s = 1 - \gamma^2. \tag{5.5}$$

The contour which passes through the saddlepoint intersects the x-axis for

$$x' = 1 + \gamma \quad \text{and} \quad x'' = 1 - \gamma. \tag{5.6}$$

According to Eqs. (2.18-21) the surface of Eq. (5.1) can also be expressed in the factored form

$$E(x, y) = (1 - \gamma^2) - [x + c_1 y^2 - (1 + \gamma)][x + c_2 y^2 - (1 - \gamma)], \tag{5.7}$$

from which, in conjunction with Eq. (5.5), it is apparent that the contours passing through the saddlepoints are the parabolas given by

$$x = (1 + \gamma) - c_1 y^2, \qquad x = (1 - \gamma) - c_2 y^2. \tag{5.8}$$

(It may be noted that, for the surfaces discussed in the preceding section, see Eq. (4.1), the first stationary condition, analogous to Eq. (5.2a), has the value (-1) on the right hand side. This leads to the solution $y_s^2 = -\gamma^2/c$ instead of Eq. (5.3). Since c is positive, it follows that there is no real saddlepoint off the x-axis, in agreement with the discussion in Sect. 4.)

The situation in this section differs from those in Sects. 3 and 4 in that, through each transition state, there passes an orthogonal trajectory which descends into the respective exit channel. Strictly speaking both trajectories originate at the reactant (here at $x = -\infty$) in agreement with the theorem that orthogonal trajectories bifurcate only at stationary points. It is therefore justified to state that bifurcation precedes the transition states. On the other hand, if the value of $|E_s|$ is small compared to $|E_R|$, with E_R being the energy of the reactant, and if y_s is small compared to $|x_R|$, the distance of the reactant from the origin, then it would seem unphysical to consider the beginning of the bifurcation at the location of the reactant. As before it would seem reasonable to consider the region preceding the VRI point as a bifurcation region. The extent of this region can perhaps be estimated by the intersection of the two straight lines which are tangent to the downhill trajectories at the two saddlepoints and which intersect on the x-axis. It is apparent that each of these straight lines is the bisectrix of the tangents to the two intersecting contours at the respective saddlepoint. These contours are given by Eq. (5.8), and, at the saddlepoints, their tangential slopes are

$$m_1 = \pm 2(\gamma + 1)\sqrt{c}, \qquad m_2 = \pm 2(\gamma - 1)\sqrt{c}, \tag{5.9}$$

where the positive signs apply when y_s is negative and the negative signs apply when y_s is positive. The slopes of the downhill trajectories at the saddlepoints are then given by $\pm m$ where m is

$$m = (1 - M_1 M_2)/(M_1 + M_2) \tag{5.10}$$

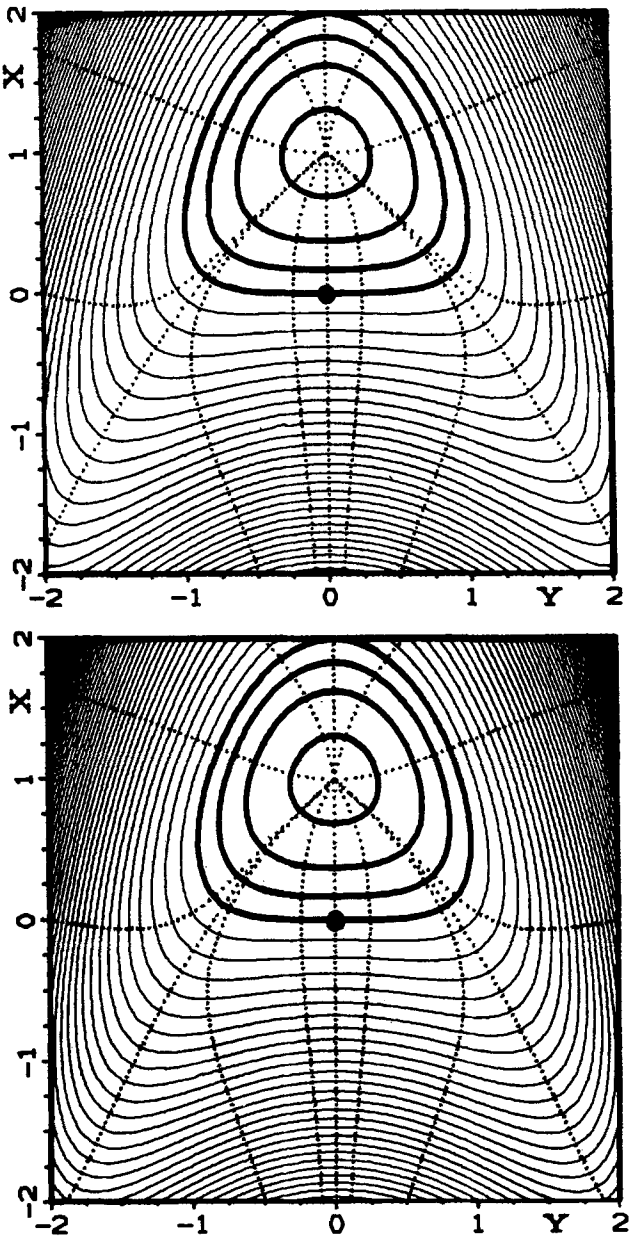

Fig. 11. *Upper panel*: the surface $E = 2x - (x + 0.5y^2)^2 = 2x - x^2 - xy^2 - 0.25y^4$. *Lower panel*: the surface $E = 2x - x^2 - xy^2 - 0.333\ldots y^4$. *Light solid lines*: contours for $E < 0$. *Heavy solid lines*: contours for $E \geq 0$. *Lowest heavy contour*: $E = 0$. Increment between *adjacent contours*: 0.3. *Dotted lines*: selected orthogonal trajectories

with

$$M_k = (1+\sqrt{1+m_k^2})/m_k, \qquad k=1,2. \tag{5.11}$$

It may be noted that m is positive when y_s is positive, and that m is negative when y_s is negative. From these slopes and the saddlepoint coordinates [Eq. (5.3)] the x-coordinate of the "bifurcation point" is found to be

$$x_B = 1-\gamma^2-|m|\gamma/\sqrt{c}. \tag{5.12}$$

It is indicated by cross marks in Figs. 9 and 10.

In the case $c_1 = -c_2$ the surface simplifies to

$$E = 2x - x^2 + c_1^2 y^2, \tag{5.13}$$

which is similar to the surface of Eq. (3.3). It differs from it only by a shift of the maximum onto the $\pm x$ axis.

Intermediate between cases $(3a)$ and $(3c)$ is case $(3b)$ where $A_4 = 0$ and $c_2 = 0$, so that

$$E(x, y) = x(2-x-c_1y^2). \tag{5.14}$$

It is readily seen that in this case the y-axis is a contour which passes through the VRI point as well as through the two saddlepoints, indeed intermediate between Figs. 9 and 10.

Figure 11a exhibits the contours for the case $(3d)$ corresponding to $A_3^2 = A_2A_4$ and $c_1 = c_2 > 0$. Figure 11b exhibits the contours for the case $(2e)$ corresponding to $A_4 < A_3^2/A_2$. In both these cases the transition states have disappeared. Only the VRI point and the maximum remain.

6. Example of a bifurcating transition region

The purpose of this section is to illustrate a bifurcating transition region on an actual reaction surface. The example we consider is the ring opening

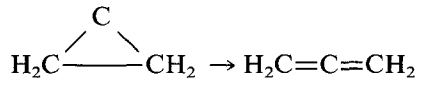

cyclopropylidene allene

a molecule with $7\times3-6=15$ internal coordinates. Of these the most important ones are ϕ = the ring-opening CCC angle at the central carbon and δ_1, δ_2 the dihedral angles between each of the CH_2 planes and the CCC plane. Figure 12 exhibits the reaction surface in terms of the two variables ϕ and $\delta = (\delta_1+\delta_2)/2$, the "average conrotatory angle". The energy is optimized with respect to all other 13 internal coordinates. The energy surface is calculated with a FORS MCSCF wavefunction [11]. There is one reactant, denoted by R, and two possible products, denoted by P_1 and P_2. It is apparent that the reaction path bifurcates near $\delta = 90°$, $\phi = 84°$ and a close-up of the surface in the neighborhood of this point is shown in Fig. 13a. It can be seen that there are two saddlepoints and a maximum between

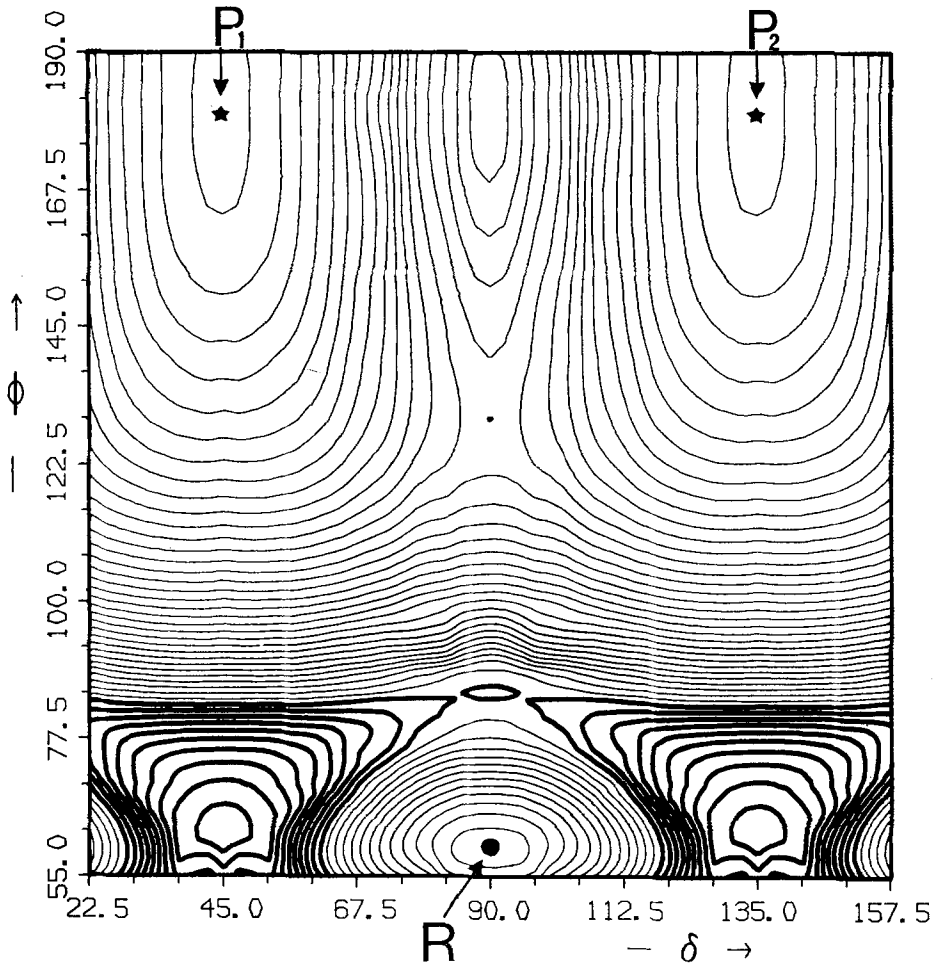

Fig. 12. The reaction surface for the ring opening of cyclopropylidene to allene. The angular coordinates are explained in the text. R = reactant = cyclopropylidene. P_1 and P_2 = the two stereoisomeric forms of the product allene. *Light solid lines*: contours for $E \leq 57.94230$ mh. *Heavy solid lines*: contours for $E \geq 62.94230$ mh. Increment between contours = 5 millihartree ≈ 3 Kcal/mole. The reactant R is the zero of energy

them, but the changes in energy between these three points are less than 0.5 mh (0.3 Kcal/mole) so that one has indeed a bifurcating transition region.

A least mean squares fit, based on 63 points, was performed in the domain indicated by the rectangle in Fig. 13a (i.e., $80° < \delta < 100°$, $82° < \phi < 88°$). It yields the expansion

$$E = -2341.024 + 56.39953\phi + 0.41866\delta^2 - 0.33074\phi^2 + 0.00000000\delta^4 - 0.0049798\phi\delta^2, \quad (6.1)$$

where the reactant, cyclopropylidene, has been arbitrarily chosen as the zero of energy and the energy unit is one millihartree. By setting $(\partial^2 E/\partial\delta^2) = 0$ for $\delta = 0$,

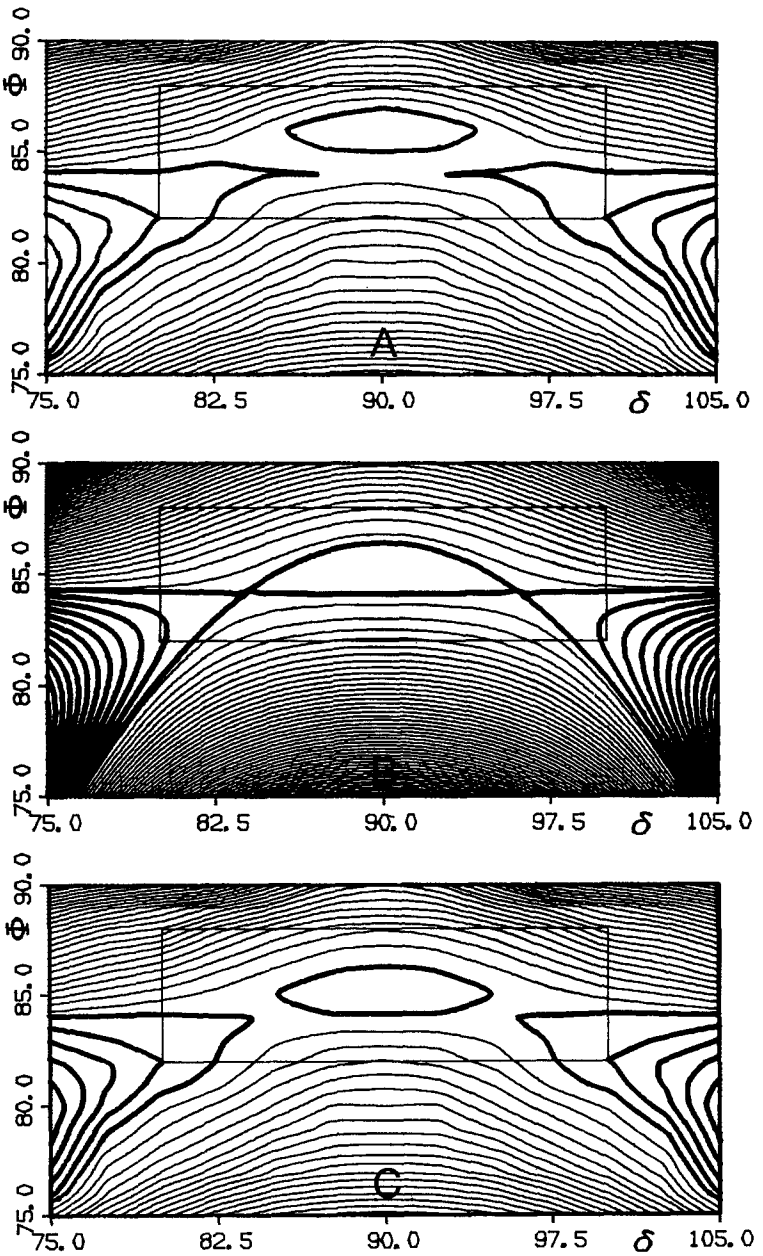

Fig. 13. Enlargement of the surface of Fig. 12 and polynomial fit in the neighborhood of the VRI Point at ($\delta = 90°$, $\phi = 84.15°$). See text in the second paragraph of Sect. 6 for details. *Light solid lines*: contours for $E \leq 62.44230$ mh. *Heavy solid lines*: contours for $E \geq 62.94230$ mh. Increment between contours = 0.5 millihartree $\approx$ 0.3 Kcal/mole

one finds the VRI point to be at ($\delta = 0$, $\phi = 84.15°$) with $E = 62.95$ mh. Appropriate shifts in ϕ and E yield the expansion in the form of Eq. (2.13) with the coefficients (in millihartree)

$$a = 0.73702, \qquad b = 0.33074,$$
$$c_1 = 0.00000, \qquad c_2 = 0.015057. \tag{6.2}$$

A measure of the closeness of the fit is obtained by dividing the value of the least mean square deviation by the mean variation of the energy in the domain over which the fit is performed. This ratio is found to be 0.04 indicating that the chosen polynomial form is germane. Figure 13b exhibits a contour plot of the polynomial fit (6.1). The fit is good within the fitted region indicated by the rectangle, but clearly inappropriate outside. Figure 13c shows the contours which are obtained by choosing values from the fit (6.1) inside the rectangle and the original raw data points outside this rectangle. This plot probably provides the best representation of the surface, because the fit (6.1) can be expected to yield the most appropriate smoothing function in the immediate neighborhood of the VRI point. (The contours in Fig. 13a were obtained by standard second order interpolation among the original data points.) From the value of the coefficients given in Eq. (6.2) it is apparent that the discussion of Sect. 5 is applicable to this problem and that one has in fact the case (3*b*), because the coefficient of δ^4 is zero within the numerical accuracy of the data.

It is evident from Fig. 13b that, with the help of the polynomial fit of Eqs. (6.1), (6.2), it is possible to determine the geometry and the energy of the transition state accurately: $\Phi = 84.24°$, $\delta = 90° \pm 5.95°$.

There exist two additional VRI points on Fig. 12, one on the line $\delta = 45°$, another on the line $\delta = 135°$, both at about $\phi = 84°$. The existence of the three VRI points and of the bifurcation is manifestly related to the fact that the alternation of maxima and minima for $\phi = 60°$ is staggered by 45° in the direction of δ with respect to the alternation of maxima and minima at 180°. For less transparent physical reasons it turns out that the VRI points at $\delta = 45°$ and 135° occur practically for the same value of ϕ as the VRI point at $\delta = 90°$. This near coincidence accounts for the fact that the straight line $\phi = 84°$ is approximately a contour which passes through all three VRI points and also through the two saddlepoints. Hence the vanishing of the coefficient of δ^4 in Eq. (6.1).

In terms of the language used in the introduction, the vanishing of A_4 is an "accident". It is therefore not unreasonable to speculate that, under other conditions, another coefficient may practically vanish. If this would be $A_1 = a$, then one would have a real situation where a point-like bifurcating transition state exists to which the discussion of Sect. 3 (case 1) is applicable.

7. Conclusions

In the present analysis valley-ridge inflection points are chosen as the basis for a discussion of bifurcations and higher-than-second-order Taylor expansions

around such points are explicitly examined. This approach leads to the identification of contour patterns which one can realistically expect to encounter on actual surfaces. The following inferences can be drawn.

The nature of bifurcations on analytical surfaces away from transition states is such that it is more reasonable to associate them with *bifurcating regions* rather than with single points.

The patterns of the energy contours near VRI points are quite different from those of a monkey saddle. Even though the entrance channel may have the character of a valley, the exit channels will more often look like watersheds than like valleys. It is possible that the exit channels contain no orthogonal trajectories that connect with the transition state. The dynamical implication is that, in the exit channels, atomic motions are more floppy than in the entrance channel.

There exists a finite, although somewhat fuzzy, domain for the values of the Taylor expansion coefficients for which there results a near-coincidence between a VRI point and a transition state. This is not a rare oddity and, in such cases, the neighborhood of a VRI point acquires the character of a *bifurcating transition region.*

If a bifurcating transition region is small enough, then it can be useful to employ the "unlikely" case 1 surface ($A_1 = 0$), corresponding to a *bifurcating transition state*, as a simplified mathematical model for the discussion of reaction mechanisms. In this case, too, the energy contour pattern is different from that of the even less likely monkey saddle.

While the present analysis assumes C_s symmetry for reasons of simplicity, corresponding topographies on more general surfaces can be visualized by applying symmetry breaking deformations to the surfaces studied here. Such deformations will not destroy the qualitative characteristics of bifurcations and transition points, so that the discussion given here for the various cases is still pertinent. In fact, a surface of this kind has been found for the ring-opening of substituted cyclopropylidenes.

While the reaction described in Sect. 6 conforms to case ($3b$), there is no reason why the other cases examined in the preceding sections should not occur on real reaction surfaces.

Acknowledgement. The authors wish to thank W. H. Miller and D. G. Truhlar for constructive criticisms of the manuscript and E. R. Davidson for a stimulating discussion.

References

1. The occurrence of bifurcations has been pointed out in a recent review article by DG Truhlar and AD Isaacson in: Clary DC (ed) Theory of chemical reaction dynamics. Reidel, Dordrecht, in press
2. Carpenter BK (1985) J Am Chem Soc. 107:5730
3. Goddard JD, Schaefer HF (1979) J Chem Phys 70:5117

4. Colwell SM (1984) Molecular physics 51:1217; Colwell SM, Handy NC (1985) J Chem Phys 82:1281
5. Tachibana A, Okazaki I, Koizumi M, Hori K, Yamabe T (1985) J Am Chem Soc 107:1190
6. Garrett B, Truhlar DG, Wagner AF, Dunning TH (1983) J Chem Phys 78:4400
7. Miller WH (1983) J Phys Chem 87:21
8. Murrell JN, Laidler K J (1968) Trans Far Soc 64:371; Murrell JN, Pratt GL (1970) Trans Far Soc 66:1680; Stanton RE, McIver JW (1975) J Am Chem Soc 97:3632; McIver JW (1974) Accounts of chemical research 7:72
9. In this statement no distinction is made between a valley and a cirque, nor between a ridge and a cliff. See [10]
10. Hoffman DK, Nord RS, Ruedenberg K (1986) Theor Chim Acta 69: 265–279
11. The details of this surface are discussed in a forthcoming publication by P. Valtazanos and K. Ruedenberg